

## Rate enhancement in the recombination of $\text{Bi}^{80+}$ ions with electrons

W. Shi, T. Bartsch, C. Böhme, C. Brandau, A. Hoffknecht, H. Knopp, S. Schippers, and A. Müller\*  
*Institut für Kernphysik, Universität Giessen, D-35392 Giessen, Germany*<sup>†</sup>

C. Kozhuharov, K. Beckert, F. Bosch, B. Franzke, P. H. Mokler, F. Nolden, M. Steck, and Th. Stöhlker  
*Gesellschaft für Schwerionenforschung (GSI), D-64291 Darmstadt, Germany*

Z. Stachura

*Institute for Nuclear Physics, 31-342 Kraków, Poland*

(Received 12 March 2002; published 27 August 2002)

Recombination of  $\text{Bi}^{80+}$  ions with electrons at low relative energies has been investigated employing the electron cooler at the experimental storage ring of the Gesellschaft für Schwerionenforschung in Darmstadt. Absolute recombination rate coefficients have been determined for relative energies  $E_{\text{rel}}$  between  $1 \times 10^{-5}$  and 10 eV. Simulations of cooling-force effects were carried out to assure the validity of these energies. In the range  $10 \text{ meV} \lesssim E_{\text{rel}} \lesssim 10 \text{ eV}$  the measured rate coefficients agree well with the theory for radiative recombination (RR). Towards lower relative energies ( $E_{\text{rel}} \lesssim 10 \text{ meV}$ ) the measured rate coefficients increasingly exceed the prediction of the RR theory. At the lowest accessible relative energy the ratio of measured and calculated rates reaches a factor of 3.5. The enhancement is found insensitive to a variation of the electron density from  $1.6 \times 10^6$  to  $4.8 \times 10^6 \text{ cm}^{-3}$ .

DOI: 10.1103/PhysRevA.66.022718

PACS number(s): 34.80.Lx, 29.20.Dh

### I. INTRODUCTION

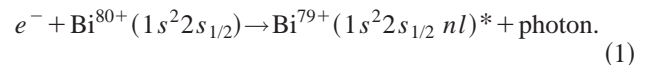
Rate enhancement in the recombination of ions with electrons at low relative energies has been an intensively investigated topic since its first observation in  $\text{U}^{28+}$  by Müller *et al.* [1] in 1991. The interest in the rate-enhancement phenomenon is largely due to the importance of understanding electron-ion recombination—one of the most fundamental atomic collision processes—and to the potential application in the production of antihydrogen by recombination of antiprotons with positrons (see reviews [2,3]). The main feature of rate enhancement is that, at very low relative energies between electrons and ions (typically  $E_{\text{rel}} \lesssim 10 \text{ meV}$ ), the measured recombination rate coefficients ( $\alpha_{\text{exp}}$ ) significantly exceed the prediction ( $\alpha_{\text{RR}}$ ) of the theory for radiative recombination (RR), while at higher energies ( $E_{\text{rel}} \gtrsim 10 \text{ meV}$ ) the measured rates can be well understood by the RR theory together with the consideration of contributions of dielectronic recombination (DR). The enhancement factor  $\epsilon = \alpha_{\text{exp}}/\alpha_{\text{RR}}$  at  $E_{\text{rel}} = 0 \text{ eV}$  ranges from  $\sim 1$  to  $\sim 400$ , depending on individual recombination processes.

While surprisingly high rate coefficients in the recombination of some multicharged complex ions such as  $\text{Au}^{25+}$  [4,5],  $\text{Au}^{50+}$  [6], and  $\text{Pb}^{53+}$  [7,8] at low relative energies can be partly traced back to DR, the enhancement phenomenon which also exists in the recombination of bare ions, where DR cannot occur, remains unexplained. Most of the previous experimental investigations for the enhancement have been devoted to light and medium-heavy few-electron or bare ions. Experiments for few-electron or bare very heavy ions (atomic number  $Z \gtrsim 80$ ) are rare due to limited availability of suitable facilities. Recently, the recombination of bare  $\text{Bi}^{83+}$

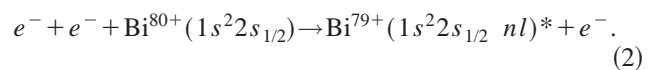
and  $\text{U}^{92+}$  ions [9,10] has been investigated in the context of rate enhancement by our collaboration using the ion-storage ring ESR at GSI in Darmstadt. The enhancement factor at cooling condition ( $E_{\text{rel}} = 0 \text{ eV}$ ) for these two ions is about 5, which is much smaller than the huge factors found in the multielectron systems mentioned above [4–8]. Therefore, it is interesting to investigate how the presence of bound electrons in the target ion influences the enhancement. In a first attempt employing lithiumlike  $\text{Bi}^{80+}$  and  $\text{U}^{89+}$  ions, surprisingly, no enhancement was observed [11]. Yet, no decisive conclusion could be drawn for  $\text{Bi}^{80+}$  and  $\text{U}^{89+}$  then, because significant nonzero angles between the electron and ion trajectories might have been involved in the experiment as a consequence of imperfections in the magnetic guiding field of the cooler. Such angles can prevent the access of relative energies lower than 10 meV, where the rate enhancement is usually observed.

After a modification of the ESR electron cooler in late 1996, a second experiment could be conducted for  $\text{Bi}^{80+}$ . This time, with much improved conditions, a rate enhancement has been observed also in the recombination of  $\text{Bi}^{80+}$ . In this paper we present the result of this experiment. Additionally, a detailed account of the correction of electron-ion relative energies due to the electron friction force is given.

The main process involved in the present work is RR, in which a free electron is captured by an ion and the excess energy and momentum are carried away by a photon:



The second possible process is three-body recombination (TBR), in which the excess energy and momentum are carried away by a second electron instead:



\*Email address: Alfred.Mueller@strz.uni-giessen.de

<sup>†</sup>URL: <http://www.strz.uni-giessen.de/~k3>

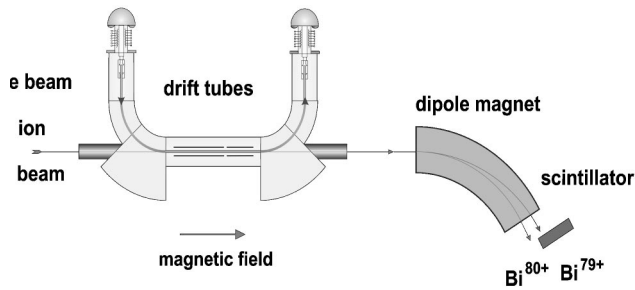


FIG. 1. Schematic view of the experimental setup. The cold electron beam produced in the gun is guided by the magnetic field and merged with the ion beam over a length of 2.5 m. The electron beam is then separated from the ion beam by the magnetic guiding field and transferred to the collector. Recombined and parent ions are separated from each other in the first dipole magnet downstream of the cooler. A scintillation detector is used to detect the recombined ions.

For  $\text{Bi}^{80+}$ , the main DR channels open up at relative energies greater than 14 eV, with the  $e + 1s^2 2s_{1/2} \rightarrow 1s^2 2p_{1/2} n l$  Rydberg resonances being energetically the lowest series. Hence, they are not involved in the energy range of the present investigation. The DR process associated with the hyperfine excitation of the core electron, though, is possible. However, as discussed in detail below it is not measurable on top of the much stronger RR process.

The present paper is arranged as follows. Experimental details are given in Sec. II. The correction of electron-ion relative energies with respect to the electron friction force is described in Sec. III. In Sec. IV experimental results are presented together with theoretical predictions. In Sec. V the main results are summarized and conclusions are drawn for the present investigation.

## II. EXPERIMENT

The main features of the experimental technique have been described in detail previously [9,10]. The measurement utilized the GSI accelerator complex. 97-MeV/u  $\text{Bi}^{80+}$  ions supplied by the combination of the linear accelerator UNILAC and the heavy-ion synchrotron SIS were injected into the ESR storage ring [12]. One injection pulse of ions from the SIS into the ESR was sufficient to provide an ion current of typically 400–800  $\mu\text{A}$  (corresponding to  $2.7 \times 10^7$ – $5.3 \times 10^7$  ions stored in the ring) at the beginning of a measurement cycle. In one of the straight sections of the ESR storage ring the ion beam was merged with the magnetically confined electron beam of the cooler (see Fig. 1).

Before starting a measurement, the ion beam was cooled for several seconds until the beam profiles reached their equilibrium widths. For a change of the electron energy, voltages between  $-5$  kV and  $+5$  kV were applied to two drift tubes surrounding the electron and ion beams in the interaction region. During a measurement cycle the electron energy was stepped through a preset range of values different from the cooling energy thus introducing nonzero mean relative velocities between the ions and the electrons. In between two measurement intervals of 40 ms duration each, the electron energy was set to the cooling energy ( $E_{\text{rel}}=0$ ) for 20 ms in

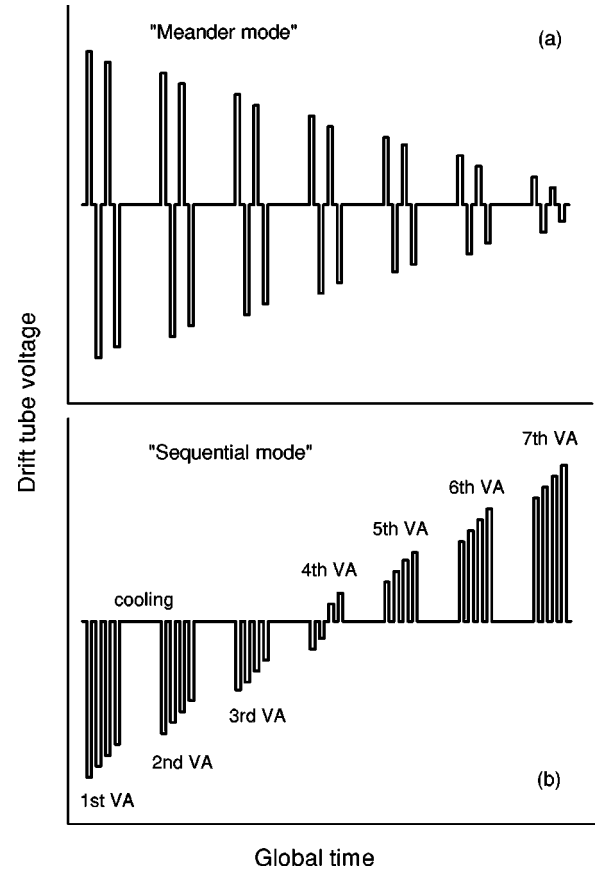


FIG. 2. Scheme of a drift-tube-voltage scan. A complete voltage scan is covered by seven virtual accelerators (VA). Each VA contains a total of 472 (instead of four shown here) alternating measurement and intermittent-cooling voltage steps. Between two adjacent VAs there is a longer cooling period (e.g., 1.5 s). The sequence of desired voltage points in a scan is arbitrary, in principle. (a) A meander mode which contains alternating positive and negative voltage steps whose height decreases from step to step. (b) A sequential mode in which the scanning of the drift-tube voltages is in a descending or ascending sequence. Drag effects on the ion beam by electron-cooling forces depend on the specific scanning scheme.

order to maintain a good ion-beam quality. A schematic representation of the timing of a complete measurement cycle is shown in Fig. 2.

Data recorded in the experiment include counts of  $\text{Bi}^{79+}$  ions on the scintillation detector (recombination detector) behind the first dipole magnet downstream the electron cooler, counts of  $\text{Bi}^{79+}$  ions on a second detector (background detector) positioned half a turn around the ring downstream the first detector (monitoring the background due to electron capture by the parent ions from the residual gas), the pulse heights of the recombination and the background detectors, the ion current, the cooler cathode voltage, the electron current, the digital and analog readouts of the drift-tube voltage, the counts of various timers and triggers, and vacuum pressures at the electron gun and at the electron collector of the cooler. The readout of the parameters was mainly triggered by a 1-kHz clock.

The space charge of the dense electron beam in the cooler reduces the energy of the electrons as nominally defined by

the cooler cathode voltage and the drift-tube voltage. The magnitude of the space-charge potential is about 80 V at cooling energy for an electron current of 300 mA. The space-charge corrected electron energy  $E_e$  and ion energy  $E_i$  are used to calculate the relative energy  $E_{\text{rel}}$  between the electron and the ion:

$$E_{\text{rel}} = \mu c^2 [\gamma_i \gamma_e - \sqrt{(\gamma_i^2 - 1)(\gamma_e^2 - 1)} \cos \theta - 1], \quad (3)$$

with  $\mu = m_e m_i / (m_e + m_i)$ ,  $\gamma_e = 1 + E_e / m_e c^2$ ,  $\gamma_i = 1 + E_i / m_i c^2$ , where  $m_e$  and  $m_i$  denote the mass of the electron and the ion, respectively,  $c$  is the speed of light, and  $\theta$  is the angle between the electron and the ion beams. Equation (3) has been derived under the assumption of  $E_{\text{rel}} \ll \sqrt{2 m_i c^2 m_e c^2}$ , which is satisfied in the present storage-ring experiments [13]. For “normal” recombination measurements the alignment of the beams is optimized to  $\theta = 0$  mrad with an uncertainty of 0.1 mrad by minimizing the width of the ion beam. This width was observed by a beam-profile monitor based on the detection of secondary ions produced by the circulating beam in the residual gas. In some experiments the angle  $\theta$  was purposely chosen different from zero in order to control the beam alignment and to check for possible effects on the rate enhancement [9].

The recombination rate coefficient  $\alpha(E_{\text{meas}})$  measured at the scanning energy  $E_{\text{meas}}$  is determined by

$$\alpha(E_{\text{meas}}) = \frac{C \gamma^2 R(E_{\text{meas}})}{\eta L n_e(E_{\text{meas}}) N_i}, \quad (4)$$

with  $R(E_{\text{meas}})$  denoting the electron-ion recombination count rate,  $\eta$  is the detection efficiency of the recombination detector, which is very close to unity,  $L = 2.5$  m is the nominal length of the interaction zone,  $n_e(E)$  is the electron density at energy  $E$ ,  $N_i$  is the number of stored ions,  $C = 108.36$  m is the ring circumference, and  $\gamma$  is the relativistic Lorentz factor for the transformation between the c.m. and the laboratory frames.

Electron and ion beams were merged and demerged by bending the electron beam in and out of the ion-beam direction using toroidal magnetic fields with a bending radius of 120 cm. The electron beam of 2.54 cm radius is still overlapping the ion beam for 25 cm before and after the straight overlap section of 250 cm. The merging and demerging sections therefore contribute to the measured counting rate. However, the influence of the voltage applied to the drift tubes is restricted to the straight overlap section of the cooler (see Ref. [9] for details) and thus, the electron energy in the toroidal sections is always the same, independent of the drift-tube potential. Therefore the contribution of the merging and demerging sections can be treated as an electron-energy-independent background.

The electrons strictly follow the magnetic-field lines. Nonzero angles between the electron trajectory and the ion-beam direction along the cooler geometrical axis are introduced by transverse components  $B_{\perp}$  of the magnetic guiding field  $B \approx B_{\parallel}$  in the merging section, whose default strength is  $B = 110$  mT. Such transverse components result from mechanical imperfections of the guiding-field-generating sole-

noid and amount to  $B_{\perp} \approx (1 \times 10^{-4}) B_{\parallel}$  in the merging region. As a result of the drift-tube voltage and interaction-angle distribution, the desired relative energy can only be realized over a certain energy-dependent fraction of the interaction length (see Refs. [9,10] for details). Thus, the measured rate coefficient at a given nominal relative energy  $E_{\text{meas}}$  contains contributions from other relative energies; i.e., it results from the convolution

$$\alpha(E_{\text{meas}}) = \frac{1}{L} \int_0^L dz \alpha(E_{\text{rel}}(z)), \quad (5)$$

with  $E_{\text{rel}}(z)$  being the relative energy at the position  $z$  inside the cooler. Accordingly, the rate coefficient  $\alpha(E_{\text{rel}})$  can therefore be obtained by a deconvolution performed iteratively (see Ref. [9]).

The systematic uncertainty of the experimental rate coefficient is estimated to be  $\pm 16\%$ . It originates from possible errors in the ion-current measurement ( $\sim \pm 5\%$ ), in the determination of the electron density ( $\sim \pm 10\%$ ), in the detection efficiency ( $\sim -5\%, +0\%$ ), and from the uncertainty of the deconvolution procedure correcting for the drift-tube potential and interaction-angle distributions ( $\sim \pm 10\%$ ). The uncertainty of the electron density was estimated on the basis of a measurement [14] in which the density of the electron beam in a cooling device was really measured and found to vary within 10%.

### III. FRICTION-FORCE CORRECTIONS

The friction force imposed on the ions by the cooling electron beam tends to drag the ions to a velocity which equals that of the electrons. Consequently, in a measurement step it shifts the relative energy between electrons and ions to a value lower than the set value. Hence, the influence of the friction force on the relative energy needs to be considered. For this purpose the evolution of the ion velocity during a measurement scan is simulated based on step-by-step (with a time increment of  $\Delta t$ ) evaluation of the ion velocity change  $\Delta v_i(t)$  due to the longitudinal friction force  $F_{\parallel}$ :

$$\Delta v_i(t) = \frac{\xi}{m_i} F_{\parallel}(t) \Delta t, \quad (6)$$

where  $\xi$  is the fractional flight time of the ion in the cooler relative to the ion circulation period in the ring.

The longitudinal cooling force at the ESR cooler was measured previously for a number of ions [15]. For the purpose of the present work the measured cooling force was represented by an appropriate continuous function of the relative velocity between the electrons and the ions. Employing Eq. (6) the ion velocity was tracked in 1-ms time steps and the real electron-ion relative energy at each step with a known nominal (set) relative energy was then found accordingly. The time resolution in the tracking of the ion velocity was varied to check for convergence of the method.

Figures 3 and 4 show the results of a simulation of the influence of the electron friction force on the recombination of  $\text{Bi}^{80+}$ . As seen from Fig. 4, for a scan of drift-tube volt-

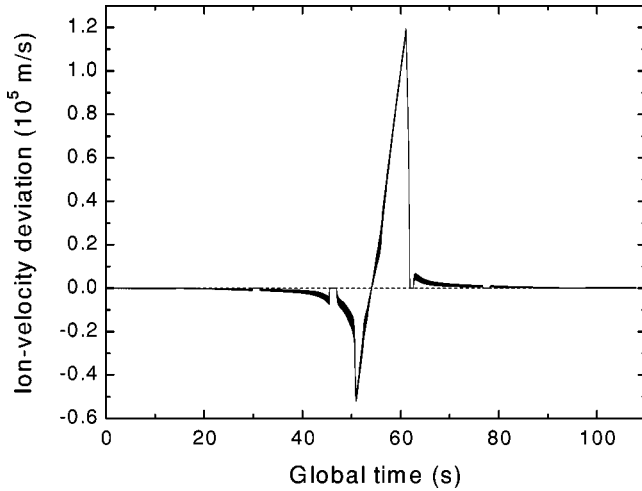


FIG. 3. Evolution of the deviation (solid line) of the  $\text{Bi}^{80+}$  ion velocity from the value at cooling simulated for a drift-tube-voltage scan from  $U_D = -2150$  V to  $U_D = +2190$  V in a sequential scheme as sketched in Fig. 2(b). The dashed line marks zero deviation as defined by the electron energy at cooling, which is nominally 53310 eV. The big features in the middle of the scan correspond to the crossing over  $U_D = 0$  V. The sharp dips and bumps (six time spans of about 1.5 s each) where the ion velocity resumes the initial velocity are due to the extended cooling between two adjacent virtual accelerators (see Fig. 2). The duration of a measurement step is 40 ms, and that of an intermittent cooling step is 20 ms. 472 voltage steps are applied during each virtual accelerator and the step sizes are equidistant in the logarithmic scale of electron-ion relative energies. The electron current is 300 mA.

ages from negative to positive in an ascending order [sequential mode, see Fig. 2(b)], the measured recombination spectrum is distorted by the friction force. However, the simulated spectrum reproduces the measured one quite well. This indicates that by tracking the development of the ion velocity we can recover the recombination spectrum with very good accuracy. It has to be pointed out that the influence of the friction force depends very much on the scan mode. By using a scan consisting of alternating positive and negative voltage steps whose height decreases from step to step [“meander mode” shown in Fig. 2(a)] or that consisting of random sampling of the voltage steps (“random mode”), the influence of the friction force can be minimized to insignificance (see Fig. 5 and compare with Fig. 3). Therefore, the meander and random scan modes were used in most of the measurements.

The present analysis shows that the effects of the cooling forces are well understood and can be accounted for in a quantitative manner. The necessity of corrections of the present energy scale for effects of the friction forces was minimized by an appropriate choice of scan modes in the present data taking scheme.

#### IV. RESULTS AND DISCUSSIONS

The drag-force corrected experimental rate coefficients and theoretical RR rate coefficients of  $\text{Bi}^{80+}$  as a function of relative energy are shown in Fig. 6.

The calculation of the RR rate coefficients is based on the

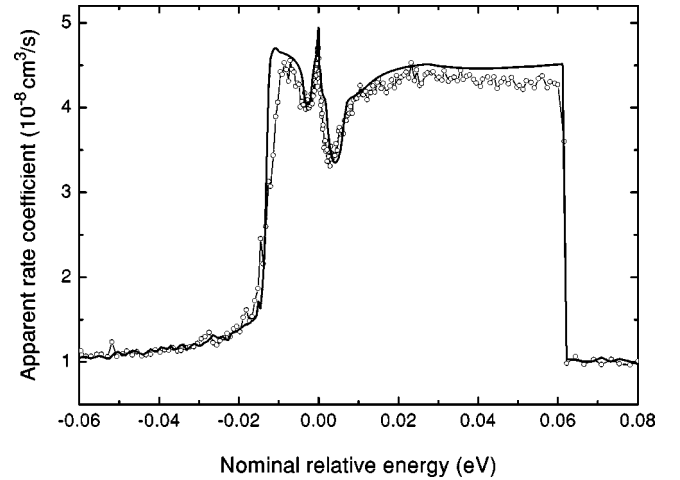


FIG. 4. Simulation of the influence of the electron friction force on the recombination of  $\text{Bi}^{80+}$  for the same voltage-scanning scheme [Fig. 2(b)] that was used to calculate the evolution of the ion velocity shown in Fig. 3. Open circles represent the measured apparent recombination rate coefficients. They are plotted as a function of the nominal relative energy. But, as a result of drag effects by the electron friction force, these rate coefficients were obtained at energies slightly different from the nominal ones. The solid line is the result of the simulation that is based on the velocity shifts displayed in Fig. 3. Negative relative energy means that the electron velocity is smaller than the ion velocity, and vice versa.

nonrelativistic quantum-mechanical dipole approximation of Stobbe [16]. According to Stobbe’s approach, the hydrogenic cross section for radiative recombination into a bound  $nl$  level is given as

$$\sigma_{nl}^{RR}(\varepsilon) = 2\pi^2 \alpha^3 a_0^2 (2l+1) \frac{1}{\varepsilon} \left( \varepsilon + \frac{1}{n^2} \right)^2 f_{nl}(\varepsilon), \quad (7)$$

where  $\alpha$  is the fine-structure constant,  $a_0$  is the Bohr radius, and  $f_{nl}(\varepsilon)$  denotes the dipole oscillator strength of a transition from the bound state  $nl$  to a continuum state with the scaled energy  $\varepsilon = E/(Z^2R)$  calculated from the energy  $E$  of the free electron, the nuclear charge  $Z$ , and the Rydberg constant  $R$ . The oscillator strength  $f_{nl}(\varepsilon)$  is evaluated, in general, by calculating the bound-continuum hydrogenic dipole matrix elements  $\langle n, l | r | \varepsilon, l \pm 1 \rangle$ , i.e.,

$$f_{nl}(\varepsilon) = \frac{1}{3(2l+1)} \left( \varepsilon + \frac{1}{n^2} \right) [ (l+1) |\langle n, l | r | \varepsilon, l+1 \rangle|^2 + l |\langle n, l | r | \varepsilon, l-1 \rangle|^2 ] \quad (8)$$

with the continuum wave functions  $|\varepsilon, l \pm 1\rangle$  being normalized to energy. For  $\text{Bi}^{80+}$  the total RR cross section is calculated by

$$\sigma^{RR}(\varepsilon) = \sum_{n,l} t_{nl} \sigma_{nl}^{RR}(\varepsilon), \quad (9)$$

where the summation  $\Sigma$  runs over all possible  $n$ ’s and  $l$ ’s, and the quantities  $t_{nl}$  are the weighting factors accounting for

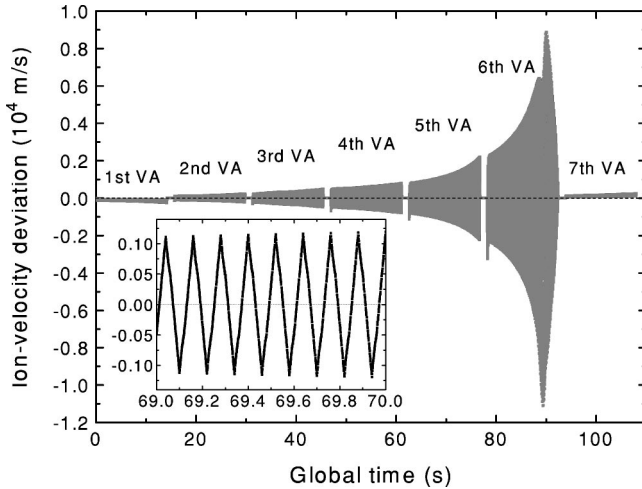


FIG. 5. Evolution of the deviation of the  $\text{Bi}^{80+}$  ion velocity from the cooling value for a voltage scan using a modified meander mode [see Fig. 2(a)]. In the scan virtual accelerators 2–6 cover the lower-energy region approaching 0 eV, where the friction force is stronger, and there the sequence of the drift-tube-voltage steps is organized in the meander mode. Virtual accelerators 1 and 7 cover the higher-energy region, where the friction force is weaker, and there the voltage steps are negative and positive voltages, respectively, in the sequence of descending amplitude as sketched in Fig. 2(b). The unresolved dots represent the simulated ion velocity deviations; the dashed line marks zero deviation as defined by the electron energy at cooling, which is nominally 53 310 eV. The gaps in between two adjacent virtual accelerators are due to extended cooling periods. The duration for a measurement step is 40 ms, and that for an intermittent cooling step is 20 ms. The simulation is for an electron current of 300 mA. The inset is an enlargement of the ion velocity evolution in the time window of 69–70 s. The maximum relative excursion of the ion velocity from its initial magnitude at cooling is about  $8 \times 10^{-5}$  as compared to  $1 \times 10^{-3}$  for the scan mode analyzed in Figs. 3 and 4.

already partially filled levels, i.e.,  $t_{10}=0, t_{20}=0.5, t_{21}=1$ , and  $t_{nl}=1$  for  $n \geq 3$ . Furthermore, in the calculation of the scaled energy,  $Z$  is replaced by the charge of the ion  $q$ , i.e.,  $\varepsilon = E/(q^2 R)$ . According to our experience, in the calculation of RR cross sections of Li-like ions,  $q$  is a good representation of the effective charge of the parent ion as seen by the recombining electron. This is in agreement with previous observation on RR of  $\text{Si}^{11+}$  [17]. For ions with more complex electronic structure, in particular, for those with partially filled shells, the effective charge can be somewhere between  $q$  and  $Z$  as shown, e.g., for the radiative recombination of  $\text{Si}^{6+}$  [17].

The contribution of Rydberg states to the measured cross section is limited by field ionization in storage-ring dipole magnets. In the simplest approach a critical quantum number  $n_{\text{max}}$  can be defined above which field ionization sets in abruptly. A useful estimate of this cutoff quantum number has been determined on the basis of calculated lifetimes of Stark states in electric fields by Müller *et al.* [18]. It is given by

$$n_{\text{max}} \approx n_{\text{F}} = \left( 7.3 \times 10^{10} \text{ V/m} \times \frac{q^3}{F} \right)^{1/4}, \quad (10)$$

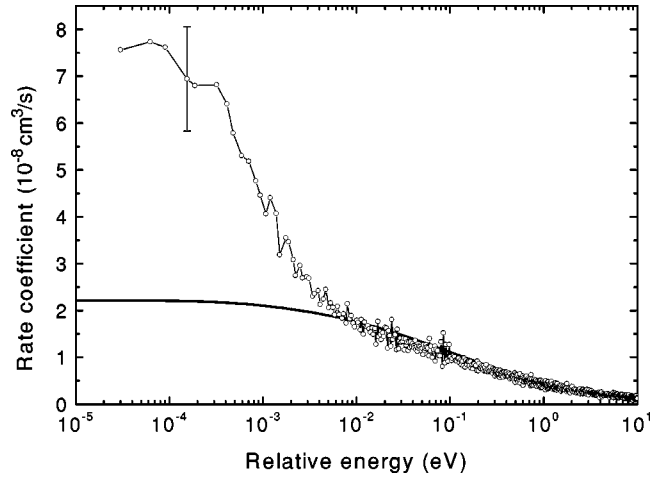


FIG. 6. Recombination rate coefficients of  $\text{Bi}^{80+}$  as a function of relative energy. Open circles represent the experiment; the solid line represents the RR theory [see Eq. (11)]. The theoretical rate coefficients were obtained by convoluting the theoretical cross sections with a flattened velocity distribution of longitudinal temperature  $kT_{\parallel}=0.4$  meV and transverse temperature  $kT_{\perp}=150$  meV. The effect of field ionization on the theoretical rates was taken into account by considering the survival probability of individual Rydberg states calculated with the detailed model for field ionization. A representative total error bar is indicated for one data point at about  $1.5 \times 10^{-4}$  eV. The scatter of the data points in the experimental spectrum originates from the deconvolution procedure [see Eq. (5)] as well as from the counting statistics particularly in the higher-energy region. Features in the rate coefficient at relative energies below  $10^{-4}$  eV cannot be resolved nor inferred from the measured data by deconvolution.

where  $F = v_i B_{\text{dip}}$  is the motional electric field seen by the ions with velocity  $v_i$  in the magnetic field  $B_{\text{dip}}$  of the dipole magnet. For the present experiment  $n_{\text{F}}=140$ . In reality, higher- $n$  Rydberg states can radiatively decay to states below  $n_{\text{F}}$  before arriving at the charge-analyzing magnet where they can be field ionized. These Rydberg ions thus can survive field ionization and be detected. In a detailed model for field ionization taking into account the effects of the radiative decay [19], the survival probability of the Rydberg ions is determined individually for each  $nl$  state populated by recombination on the basis of hydrogenic radiative decay rates and field-ionization rates. In the present work this detailed model has been applied to the calculation of the RR cross sections with the experimental field-ionization effect being accounted for.

For the comparison with the merged-beam rate coefficients, the theoretical cross sections were convoluted with the experimental electron-velocity distribution function  $f(v_{\text{rel}}, \mathbf{v})$  characterized by the temperatures  $kT_{\parallel}$  and  $kT_{\perp}$  parallel and perpendicular to the electron-beam direction, respectively, resulting in the theoretical rate coefficients  $\alpha^{\text{RR}}(E_{\text{rel}})$ :

$$\alpha^{\text{RR}}(E_{\text{rel}}) = \sum_{n,l} Y_{nl} t_{nl} \int \sigma_{nl}^{\text{RR}}(v) v f(v_{\text{rel}}, \mathbf{v}) d^3 \mathbf{v}, \quad (11)$$

where  $Y_{nl}$  is the survival probability of the Rydberg state

characterized by quantum numbers  $n$  and  $l$ , and  $v_{\text{rel}}$  is the difference of mean longitudinal velocities between the electrons and the ions or, in other words, the detuning velocity, which is related to  $E_{\text{rel}}$  by  $E_{\text{rel}} = \mu v_{\text{rel}}^2/2$ . The longitudinal temperature  $kT_{\parallel}$  was inferred from the analysis of  $\text{Bi}^{80+}$  DR peaks at resonance energies above 200 eV measured during this experiment at the ESR. The observed peak shapes can be reproduced assuming  $kT_{\parallel} = (0.4 \pm 0.1)$  meV [20] for the present measurement. On the basis of a comparison of theory and experiment (see Fig. 6) at energies above  $10^{-2}$  eV, the transverse temperature  $kT_{\perp}$  is estimated to be 150 meV, which is not much different from the lower limit (120 meV) determined by the cooler cathode temperature.

We point out that fully relativistic calculations of radiative recombination are available for bare ions with  $n \leq 3$  [21]. As explained in more detail in Refs. [9,10] relativistic effects can be as large as about 10% for cross sections of recombination into an individual shell. However, they largely cancel out even for  $\text{U}^{92+}$  ions when total cross sections are considered. Therefore, the relativistic effects are neglected here.

As can be seen from Fig. 6, for relative energies greater than 10 meV, the measured rate coefficients agree very well with the RR theory. For relative energies below 10 meV ( $E_{\text{rel}} \leq 10$  meV) the measured rate coefficients exceed the RR theory. As the relative energy decreases, the difference becomes larger and finally levels off. At the lowest accessible energy the measured rate coefficient amounts to  $7.7 \times 10^{-8} \text{ cm}^3 \text{ s}^{-1}$ , exceeding the theoretical one of  $2.2 \times 10^{-8} \text{ cm}^3 \text{ s}^{-1}$  by a factor of 3.5.

To quantify the rate enhancement, one often uses the excess rate  $\Delta\alpha$ , which is defined as the difference of rate coefficients from experiment and RR theory, i.e.,  $\Delta\alpha = \alpha_{\text{exp}} - \alpha_{\text{RR}}$ . The excess rate was found by Gwinner *et al.* [22] to scale with the transverse electron temperature as  $T_{\perp}^{-1/2}$  and with the longitudinal electron temperature as  $T_{\parallel}^{-1/2}$ . In order to compare the rate enhancement of the few-electron ion  $\text{Bi}^{80+}$  with that of bare  $\text{Bi}^{83+}$  and  $\text{U}^{92+}$  ions more quantitatively, we look at electron-temperature-scaled excess rates  $\Delta\alpha(kT_{\perp})^{1/2}(kT_{\parallel})^{1/2}$ . In Fig. 7 the scaled excess rate at  $E_{\text{rel}} = 0$  eV for the recombination of  $\text{Bi}^{80+}$  together with those for bare ions including  $\text{Bi}^{83+}$  and  $\text{U}^{92+}$  measured previously is displayed. Also shown in the figure is the ion-charge scaling of scaled excess rates  $\sim q^{2.6}$  found first by Gao *et al.* [24] for light bare ions and then extended by Shi *et al.* [10] to the heaviest bare ions. The figure shows that the scaled excess rate for  $\text{Bi}^{80+}$  fits well to the ion-charge scaling found for bare ions. This seems to indicate that the bound electrons of  $\text{Bi}^{80+}$  are not critical to the enhancement besides occupying possible capture states and opening up DR channels above certain thresholds. For nonbare ions one might also plot the scaled excess rate as a function of the effective charge of the ion. Then the data point for  $\text{Bi}^{80+}$  would move towards a higher charge state and would then fit better to the scaling for bare ions. The uncertainty of the present scaled excess rate for  $\text{Bi}^{80+}$ , however, does not permit a more detailed conclusion.

In order to investigate mechanisms possibly causing the enhancement, the electron density has been varied and cor-

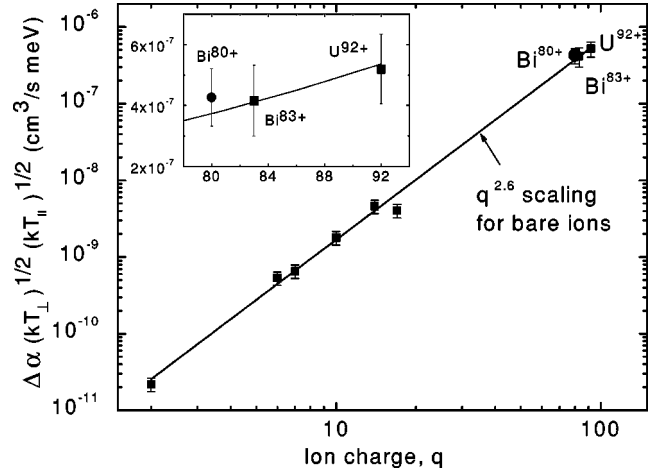


FIG. 7. Scaled excess rates  $\Delta\alpha(kT_{\perp})^{1/2}(kT_{\parallel})^{1/2}$  at 0 eV in the recombination of  $\text{Bi}^{80+}$  and of bare ions. The filled circle represents  $\text{Bi}^{80+}$ , and the full squares are for bare ions measured previously using storage rings [9,10,22–26]. The error bar indicated for  $\text{Bi}^{80+}$  includes contributions from the uncertainty of the excess rate and that of  $kT_{\parallel}$  and  $kT_{\perp}$ . The solid line is the  $q^{2.6}$  scaling of scaled excess rates for the recombination of bare ions found previously [10,24]. The inset is an enlargement of the heaviest ions.

responding recombination spectra were measured. In Fig. 8 the recombination rate at the minimum accessible energy ( $E_{\text{rel}} = 0$  eV) has been plotted as a function of the electron density. Obviously, the rate coefficients at the three different electron densities are the same within the error bars. In fact, even the detailed recombination spectra for different electron densities are essentially identical in the energy range  $10^{-5} \text{ eV} \leq E_{\text{rel}} \leq 10$  eV. The independence of the enhancement of the electron density, which was also observed previously in the recombination of ions such as  $\text{Bi}^{83+}$  [9] and  $\text{F}^{6+}$  [22], rules out TBR as a possible explanation for the enhancement. The TBR process would show a strong dependence on the electron density.

In the recombination of  $\text{Bi}^{83+}$  [9] and  $\text{U}^{92+}$  [10], which were carried out also at the ESR but with a much higher ion energy of  $\sim 300$  MeV/u, the measured recombination rates at very low relative energies were observed to oscillate with the magnetic guiding field strength, which has never been observed in recombination experiments carried out at other storage rings. Here, for  $\text{Bi}^{80+}$  in an additional measurement the magnetic guiding field strength was also varied, however, no such oscillations have been observed. While the oscillatory behavior observed in  $\text{Bi}^{83+}$  and  $\text{U}^{92+}$  has not been fully understood so far, we speculate that the different behavior in the dependence of low-energy recombination rates on the magnetic guiding field strength between  $\text{Bi}^{80+}$  and  $\text{Bi}^{83+}$  and  $\text{U}^{92+}$  might be due to the substantial difference in the experimental ion energies. This speculation is based on the additional transverse cyclotron motion of electrons in the ESR cooler due to nonadiabatic relaxation of the electron beam during fast acceleration to some 100 keV in a short gap of 15 cm length and its strong dependence on the electron energy. The additional transverse velocity  $v_c$  introduced by the acceleration is proportional to  $E_e^{2.8}$  [15]. At an ion energy of 100 MeV/u (thus  $E_e \sim 50$  keV) the transverse velocity of the

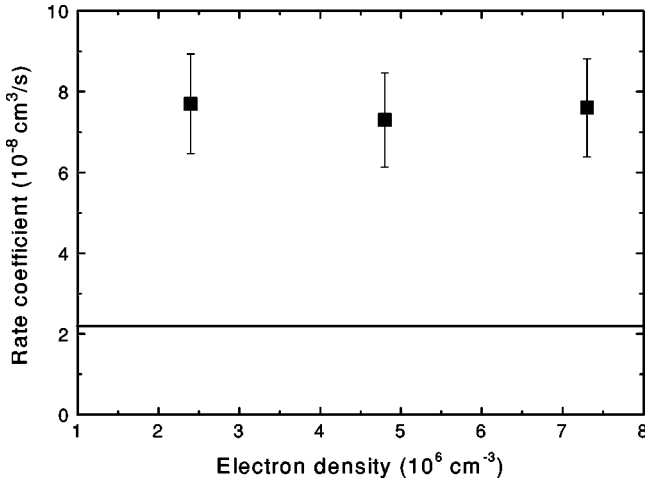
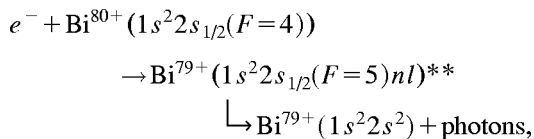


FIG. 8. Dependence of the rate coefficient at  $E_{\text{rel}}=0$  eV on the electron density for the recombination of  $\text{Bi}^{80+}$ . Full squares represent the experiment; the solid line is the RR theory of Eq. (11). The theoretical rate coefficient was calculated with  $kT_{\parallel}=0.4$  meV and  $kT_{\perp}=150$  meV. The effect of field ionization on the theoretical rate was taken into account by considering the survival probability of individual Rydberg states calculated with the detailed model for field ionization. As indicated by the error bars, an uncertainty of  $\pm 13\%$  is quoted for the experimental rate coefficients.

additional cyclotron motion is about an order of magnitude smaller than the mean thermal transverse velocity  $\langle v_{e\perp} \rangle$ , while at an ion energy of 300 MeV/u ( $E_e \sim 160$  keV) the transverse velocity of the additional cyclotron motion is much larger than the mean thermal transverse velocity, so that at the ion energy of 300 MeV/u the transverse electron motion is dominated by the additional cyclotron motion, which is not the case at the lower ion energy and at electron coolers of other ion-storage rings operating at much lower energies. The additional cyclotron motion might be the cause for the oscillations observed in the measurements carried out at higher ion energies. This, however, does not mean that the additional cyclotron motion is the cause of the rate enhancement itself.

As the ground state  $1s^2 2s_{1/2}$  of the  $^{209}\text{Bi}^{80+}$  ion is split into two hyperfine components with a total angular momentum of  $F=4$  and  $F=5$ , respectively, the DR process associated with the hyperfine excitation of the core electron ( $F=4 \rightarrow F=5$ ),



is energetically possible in the present energy region, and hence, its role in the observed rate enhancement needs to be discussed.

The hyperfine splitting of the ground state is about 0.8 eV as was measured [27] and predicted (see, e.g., Ref. [28]) previously. The resulting DR resonances associated with the hyperfine excitation should exhibit a resonance series of the type  $1s^2 2s_{1/2}(F=5)nl$  with a series limit at about 0.8 eV.

The lowest energetically allowed resonance in the series corresponds to  $n \approx 330$ . However, all states in the series are field ionized in the dipole magnet behind the electron cooler, which sets in at a field-ionization cutoff quantum number  $n_{\text{max}} = n_F \approx 140$ . At most, when the radiative stabilization of higher Rydberg states on the way between the cooler and the magnetic dipole field that causes field ionization is taken into account, one might expect a detection limit of higher- $n$  Rydberg states at  $n_{\text{max}} \approx 320$  as indicated by the detailed model calculation for the survival probability of the Rydberg states. Also, the cross section for the DR associated with the  $F=4 \rightarrow F=5$  hyperfine excitation has to be expected to be orders of magnitude smaller than that of the radiative recombination, as is the case for  $\text{Bi}^{82+}$  ions [29]. Therefore, we conclude that DR associated with the hyperfine excitation of the core electron did not produce a significant contribution to the enhanced rates measured in this experiment at very low energies. This does not preclude the possibility to study that mechanism in a separate dedicated experiment with suitably chosen conditions.

## V. SUMMARY AND CONCLUSIONS

In conclusion, absolute rate coefficients for the recombination of  $\text{Bi}^{80+}$  with electrons have been measured for relative energies between  $1 \times 10^{-5}$  and 10 eV. A very good agreement of the measured rate coefficients with the predictions of the RR theory is obtained at energies higher than 10 meV. A model simulation of drag-force effects on the ion beam is presented. In conjunction with the experiment the simulation shows that drag-force effects can be minimized by choosing appropriate energy-scan schemes. The simulations were used to assure the validity of the energy scale of the measured recombination rates.

A low-energy rate enhancement has been observed in the recombination of  $\text{Bi}^{80+}$ . The rate coefficient at the minimum accessible relative energy is 3.5 times that predicted by the RR theory. The enhancement of the few-electron ion  $\text{Bi}^{80+}$  fits well to the ion-charge scaling found for bare ions including  $\text{Bi}^{83+}$  and  $\text{U}^{92+}$ . This indicates that the bound electrons of  $\text{Bi}^{80+}$  are not critical to the enhancement besides occupying possible states and opening up DR channels above certain thresholds. The lack of a dependence of the enhancement on the electron density excludes TBR as the enhancement mechanism. Dielectronic recombination associated with the hyperfine excitation of the core electron of  $\text{Bi}^{80+}$  should not play any significant role in the observed enhancement.

## ACKNOWLEDGMENTS

The Giessen group gratefully acknowledges support for this work through Contract Nos. GI-MUL S and GI-MUL A with the Gesellschaft für Schwerionenforschung (GSI), Darmstadt, and by research grants (Nos. 06 GI 848 and 06 GI 947) from the Bundesministerium für Bildung und Forschung (BMBF), Bonn.

- [1] A. Müller, S. Schennach, M. Wagner, J. Haselbauer, O. Uwira, W. Spies, E. Jennewein, R. Becker, M. Kleinod, U. Pröbstel, N. Angert, J. Klabunde, P.H. Mokler, P. Spädtke, and B. Wolf, *Phys. Scr.*, **T37**, 62 (1991).
- [2] M.H. Holzscheiter and M. Charlton, *Rep. Prog. Phys.* **62**, 1 (1999).
- [3] G. Gabrielse, in *Advances in Atomic, Molecular and Optical Physics*, edited by B. Bederson and H. Walther (Academic Press, San Diego, 2001) Vol. 45, p. 1.
- [4] A. Hoffknecht, O. Uwira, S. Schennach, A. Frank, J. Haselbauer, W. Spies, N. Angert, P.H. Mokler, R. Becker, M. Kleinod, S. Schippers, and A. Müller, *J. Phys. B* **31**, 2415 (1998).
- [5] G.F. Gribakin, A.A. Gribakina, and V.V. Flambaum, *Aust. J. Phys.* **52**, 443 (1999).
- [6] O. Uwira, A. Müller, J. Linkemann, T. Bartsch, C. Brandau, M. Schmitt, A. Wolf, D. Schwalm, R. Schuch, W. Zong, H. Lebius, W.G. Graham, J. Doerfert, and D.W. Savin, *Hyperfine Interact.* **108**, 149 (1997).
- [7] S. Baird, J. Bosser, C. Carli, M. Chanel, P. Levèvre, R. Ley, R. Maccaferri, S. Maury, I. Meshkov, D. Möhl, G. Molinari, F. Motsch, H. Mulder, G. Tranquille, and F. Varenne, *Phys. Lett. B* **361**, 184 (1995).
- [8] E. Lindroth, H. Danared, P. Glans, Z. Pesic, M. Tokman, G. Viktor, and R. Schuch, *Phys. Rev. Lett.* **86**, 5027 (2001).
- [9] A. Hoffknecht, C. Brandau, T. Bartsch, C. Böhme, H. Knopp, S. Schippers, A. Müller, C. Kozhuharov, K. Beckert, F. Bosch, B. Franzke, A. Krämer, P.H. Mokler, F. Nolden, M. Steck, Th. Stöhlker, and Z. Stachura, *Phys. Rev. A* **63**, 012702 (2001).
- [10] W. Shi, S. Böhm, C. Böhme, C. Brandau, A. Hoffknecht, S. Kieslich, S. Schippers, A. Müller, C. Kozhuharov, F. Bosch, B. Franzke, P.H. Mokler, M. Steck, Th. Stöhlker, and Z. Stachura, *Eur. Phys. J. D* **15**, 145 (2001).
- [11] W. Spies, A. Müller, O. Uwira, B. Franzke, C. Kozhuharov, P.H. Mokler, M. Steck, Th. Winkler, and M.S. Pindzola, *Hyperfine Interact.* **108**, 155 (1997).
- [12] B. Franzke, *Nucl. Instrum. Methods Phys. Res. B* **24/25**, 18 (1987).
- [13] W. Spies, Ph.D. thesis, Universität Giessen, Giessen 1995 (unpublished).
- [14] L.H. Andersen, J. Bolko, and P. Kvistgaard, *Phys. Rev. A* **41**, 1293 (1990).
- [15] T. Winkler, K. Beckert, F. Bosch, H. Eickhoff, B. Franzke, F. Nolden, H. Reich, B. Schlitt, and M. Steck, *Nucl. Instrum. Methods Phys. Res. A* **391**, 12 (1997).
- [16] M. Stobbe, *Ann. Phys. (Leipzig)* **7**, 661 (1930).
- [17] L.H. Andersen, G.Y. Pan, and H. Schmidt, *J. Phys. B* **25**, 277 (1992).
- [18] A. Müller, D.S. Belić, B.D. DePaola, N. Djurić, G.H. Dunn, D.W. Mueller, and C. Timmer, *Phys. Rev. A* **36**, 599 (1987).
- [19] S. Schippers, A. Müller, G. Gwinner, J. Linkemann, A.A. Saghiri, and A. Wolf, *Astrophys. J.* **555**, 1027 (2001).
- [20] W. Shi, T. Bartsch, C. Böhme, C. Brandau, A. Hoffknecht, H. Knopp, S. Schippers, A. Müller, T. Steih, N. Grün, W. Scheid, C. Kozhuharov, F. Bosch, B. Franzke, P.H. Mokler, M. Steck, Th. Stöhlker, and Z. Stachura (unpublished).
- [21] A. Ichihara and J. Eichler, *At. Data Nucl. Data Tables* **74**, 1 (2000).
- [22] G. Gwinner, A. Hoffknecht, T. Bartsch, M. Beutelspacher, N. Eklöw, P. Glans, M. Grieser, S. Krohn, E. Lindroth, A. Müller, A.A. Saghiri, S. Schippers, U. Schramm, D. Schwalm, M. Tokman, G. Wissler, and A. Wolf, *Phys. Rev. Lett.* **84**, 4822 (2000).
- [23] H. Gao, D.R. DeWitt, R. Schuch, W. Zong, S. Asp, and M. Pajek, *Phys. Rev. Lett.* **75**, 4381 (1995).
- [24] H. Gao, R. Schuch, W. Zong, E. Justiniano, D.R. DeWitt, H. Lebius, and W. Spies, *J. Phys. B* **30**, L499 (1997).
- [25] H. Gao, S. Asp, C. Biedermann, D.R. DeWitt, R. Schuch, W. Zong, and H. Danared, *Hyperfine Interact.* **99**, 301 (1996).
- [26] A. Hoffknecht, S. Schippers, A. Müller, G. Gwinner, D. Schwalm, and A. Wolf, *Phys. Scr.*, **T92**, 402 (2001).
- [27] P. Beiersdorfer, A.L. Osterheld, J.H. Scofield, J.R. Crespo López-Urrutia, and K. Widmann, *Phys. Rev. Lett.* **80**, 3022 (1998).
- [28] J. Sapirstein and K.T. Cheng, *Phys. Rev. A* **63**, 032506 (2001).
- [29] M.S. Pindzola, N.R. Badnell, and D.C. Griffin, *Phys. Rev. A* **45**, R7659 (1992).